

# Transverse Spin Effects In Diffractive Hadron Leptoproduction

S.V.Goloskokov <sup>1</sup>

Bogoliubov Laboratory of Theoretical Physics,  
Joint Institute for Nuclear Research.  
Dubna 141980, Moscow region, Russia.

## Abstract

We consider double spin asymmetries for longitudinally polarized leptons and transversally polarized protons in diffractive vector meson and  $Q\bar{Q}$  production at high energy range on the basis of two-gluon model. The asymmetry predicted for meson production is quite small. Large asymmetry is expected for  $Q\bar{Q}$  production.

---

<sup>1</sup>Email: goloskkv@thsun1.jinr.ru

# 1 Introduction

Study of the hadron structure is a fundamental problem of modern physics. One of the important object here is a parton distributions in a nucleon. The cross section of inclusive hadron production is expressed in terms of ordinary parton distributions where partons have the same momenta. The more general structure - skewed parton distributions (SPD) [1, 2] in a nucleon can be studied in diffractive hadron leptoproduction. Diffractive reactions have the same particle (proton e.g.) in initial and final state and the  $t$  channel exchange is colorless. In the diffractive vector meson and  $Q\bar{Q}$  production, the nonzero momentum  $x_P$  carried by the two-parton system appears and the parton momenta cannot be equal. It have been found that the amplitude of such process factorizes into a hard subprocess and a soft proton matrix element- SPD [3]. The diffractive charm  $Q\bar{Q}$  production and  $J/\Psi$  production are determined by the gluon SPD  $\mathcal{F}_\zeta(x)$  because the charm component in the proton is small. The processes with the light quarks are predominated at small Bjorken  $x \leq 0.1$  by the Pomeron exchange which can be associated with two gluon state [4]. Both quark and gluon SPD will contribute here for  $x > 0.1$ .

Sensitivity of diffractive lepto and photoproduction to the gluon density in the proton gives an excellent tool to test these structure functions. Intensive experimental study of diffractive processes were performed in DESY [5, 6, 7, 8]. Study of the longitudinal double spin asymmetry has been performed in [9]. Theoretical investigation of the diffractive vector meson production was done on the basis of different models. Within two- gluon exchange model it was found that the typical scale variable for different vector mesons is determined by  $\bar{Q}^2 = (Q^2 + M_V^2)/4$  [10, 11]. In papers [12, 13, 14] analyses of the cross section for longitudinal and transverse photon polarization was done. It was shown that longitudinally polarized photon gives predominated contribution to the cross section for  $Q^2 \rightarrow \infty$ . The cross section with transverse photon polarization is suppressed as power of  $Q$ . Investigation of the vector meson production within SPD approach was performed by many authors (see e.g [15, 16]). Within SPS approach one has possibility to study simultaneously the imaginary and real parts of the diffractive amplitudes. In paper [17] the double spin asymmetry for longitudinal photon and proton polarization in vector meson production was estimated.

Theoretical analyses of the diffractive  $Q\bar{Q}$  pares production which can be observed as two jet events in lepton proton interaction has been done e.g. in [18, 19, 20]. In these papers cross sections are expressed in terms of gluon distributions as in the case of vector meson production. Spin effects in diffractively produced quark-antiquark pare for longitudinally polarized lepton and proton was discussed in [21] in order to analyze

diffractive contribution to  $g_1$  structure function.

Thus the diffractive reactions should play a key role in study of gluon structure of the proton at small  $x$ . In the case of polarized particles the spin-dependent gluon distributions can be investigated. In most papers spin asymmetries for longitudinally polarized particles were analyzed. In future it will be an excellent possibility to study spin effects with transversally polarized target at HERMES. Such experiment should shed a light on the polarized parton distributions, which are responsible on the transverse, spin effects in the hadron.

In this paper we consider double spin asymmetries for longitudinally polarized leptons and transversally polarized protons in diffractive vector meson and  $Q\bar{Q}$  production at high energies. Some preliminary results in this field was published in [22]. The two-gluon exchange model with the spin-dependent  $gg$ -proton coupling is used. This means that that our results should be applicable for reactions with heavy quarks which are determined by the gluons exchange. For processed with light quarks our predictions should be valid at small  $x$  region ( $x \leq 0.1$  e.g.). The cross section of the hadrons leptoproduction can be decomposed into the leptonic and hadronic tensors and the amplitude of the hadron production through the  $\gamma^*gg$  transition to the vector meson or  $Q\bar{Q}$  states. After describing the kinematics of the process in Sect. 2, we analyze the structure of the leptonic and hadronic tensors in Sect. 3. In Sect. 4, we calculate the polarized cross section of the vector meson leptoproduction. Connection of two-gluon approach with skewed gluon distributions is discussed too. Similar results for diffractive  $Q\bar{Q}$  production is presented in Sect. 5. The numerical results for the diffractive vector meson and production at HERA and HERMES energies and our prediction to the  $A_{lT}$  asymmetry can be found in Sect 6 and 7. We finish with the concluding remarks in Sect. 8.

## 2 Kinematics of Diffractive Hadron Leptoproduction

Let us study the diffractive hadron production in lepton-proton reactions

$$l + p \rightarrow l + p + H \quad (1)$$

at high energies in lepton-proton system. The hadron state  $H$  in this reaction can contains vector meson or  $Q\bar{Q}$  system which can be detected as two final jets. The reaction (1) can be described in terms of the kinematic variables which are defined as follows:

$$\begin{aligned} q^2 &= (l - l')^2 = -Q^2, \quad t = r_P^2 = (p - p')^2, \\ y &= \frac{p \cdot q}{l \cdot p}, \quad x = \frac{Q^2}{2p \cdot q}, \quad x_P = \frac{q \cdot (p - p')}{q \cdot p}, \quad \beta = \frac{x}{x_P}, \end{aligned} \quad (2)$$

where  $l, l'$  and  $p, p'$  are the initial and final lepton and proton momenta, respectively,  $q = l - l'$ ,  $Q^2$  is the photon virtuality and  $r_P$  is a momentum carried by the Pomeron. The last variable  $\beta$  is used in  $Q\bar{Q}$  production. In this case the effective mass of produced quark system is equal to  $M_X^2 = (q + r_P)^2 \sim x_P y p_+^2 - Q^2 + t$  and may be quite large. The new variable  $\beta = x/x_P \sim Q^2/(M_X^2 + Q^2)$  which appears in this case can vary from 0 to 1. For diffractive vector meson production  $M_X^2 = M_V^2$  and  $\beta \sim 1$  for large  $Q^2$ . From the mass-shell equation for vector-meson momentum  $K_V^2 = (q + r_P)^2 = M_V^2$  we find that for these reactions

$$x_P \sim \frac{m_V^2 + Q^2 + |t|}{sy} \quad (3)$$

and is small at high energies. This variable does not fix for  $Q\bar{Q}$  production.

We use the light-cone variables that are determined as  $a_{\pm} = a_0 \pm a_z$ . In these variables the scalar production of two 4-vectors look like

$$a \cdot b = \frac{1}{2}(a_+ b_- + a_- b_+) - \vec{a}_\perp \vec{b}_\perp,$$

where  $\vec{a}_\perp$  and  $\vec{b}_\perp$  represent the transverse parts of the momenta. In calculation the center of mass system is used where the momenta of the initial lepton and proton are going along the  $z$  axis and have the form

$$l = (p_+, \frac{\mu^2}{p_+}, \vec{0}), \quad p = (\frac{m^2}{p_+}, p_+, \vec{0}). \quad (4)$$

Here  $\mu$  and  $m$  are the lepton and proton mass. The energy of the lepton-proton system then reads as  $s \sim p_+^2$ . We can determine the spin vectors with positive helicity of the lepton and the proton by

$$\begin{aligned} s_l &= \frac{1}{\mu}(p_+, -\frac{\mu^2}{p_+}, \vec{0}), \quad s_l^2 = -1, \quad s_l \cdot l = 0; \\ s_p &= \frac{1}{m}(\frac{m^2}{p_+}, -p_+, \vec{0}), \quad s_p^2 = -1, \quad s_p \cdot p = 0. \end{aligned} \quad (5)$$

The polarization vector for transversally polarized target can be written in the form

$$s_p^\perp = (0, 0, \vec{s}_\perp), \quad \vec{s}_\perp^2 = 1. \quad (6)$$

The momenta are carried by the photon and the Pomeron and can be written as follows:

$$\begin{aligned} q &= (y p_+, -\frac{Q^2}{p_+}, \vec{q}_\perp), \quad |q_\perp| = \sqrt{Q^2(1-y)}, \quad \text{and} \quad q^2 = -Q^2; \\ r_P &= (-\frac{|t|}{p_+}, x_P p_+, \vec{r}_\perp), \quad |r_\perp| = \sqrt{|t|(1-x_P)}, \quad \text{and} \quad r_P^2 = t. \end{aligned} \quad (7)$$

### 3 Structure of Leptonic and Hadronic Tensors

#### 3.1 Leptonic Tensor

The structure of the leptonic tensor is quite simple [23] because the lepton is a point-like object

$$\begin{aligned}\mathcal{L}^{\mu\nu}(s_l) &= \sum_{\text{spin } s_f} \bar{u}(l', s_f) \gamma^\mu u(l, s_l) \bar{u}(l, s_l) \gamma^\nu u(l', s_f) \\ &= \text{Tr} \left[ (l + \mu) \frac{1 + \gamma_5 s_l}{2} \gamma^\nu (l' + \mu) \gamma^\mu \right].\end{aligned}\quad (8)$$

Here  $l$  and  $l'$  are the initial and final lepton momenta, and  $s_l$  is a spin vector of the initial lepton determined in (5).

The sum and difference of the cross sections with parallel and antiparallel longitudinal polarization of a proton and a lepton are expressed in terms of the spin-average and spin-dependent hadron and lepton tensors. The latter is determined by the relation

$$\mathcal{L}^{\mu\nu}(\pm) = \frac{1}{2} (\mathcal{L}^{\mu\nu}(+\frac{1}{2}) \pm \mathcal{L}^{\mu\nu}(-\frac{1}{2})), \quad (9)$$

where  $\mathcal{L}^{\mu\nu}(\pm\frac{1}{2})$  are the tensors with the helicity of the initial lepton equal to  $\pm 1/2$ . The tensors (9) look like

$$\begin{aligned}\mathcal{L}^{\mu\nu}(+) &= 2(g^{\mu\nu}l \cdot q + 2l^\mu l^\nu - l^\mu q^\nu - l^\nu q^\mu), \\ \mathcal{L}^{\mu\nu}(-) &= 2i\mu\epsilon^{\mu\nu\delta\rho}q_\delta(s_l)_\rho.\end{aligned}\quad (10)$$

#### 3.2 Proton Two Gluon Coupling and Hadron Tensor

The  $Q\bar{Q}$  system which appears in the final state or going to the vector meson in reaction (1) can be produced by two ways. The first one is the photon interaction with the  $Q\bar{Q}$  state from the proton. This contribution can be connected with the quark distribution in a nucleon. The other contribution is determined by the photon-gluon fusion which produces  $Q\bar{Q}$  system. The quark pair must be in color singlet state to produce the vector meson. This means that gluon state should be colorless too and contains two gluons at least. We are working in the low  $x$  region, where gluon contribution is predominated. It is associated with the Pomeron that describes diffractive processes at high energies. In a QCD inspired models the Pomeron is usually represented as two-gluon object.

Properties of gluon structure function is determined by the non-perturbative effects inside the proton. We shall analyze the matrix structure of two-gluon coupling with the proton within the quark-diquark model [24] where the proton is being composed of a quark

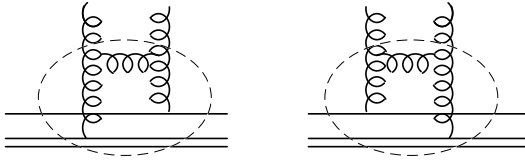


Figure 1: Graphs which give leading Log contribution to  $ggp$  vertex in  $\alpha^2$  order.

and a diquark. The composite scalar and vector diquarks provide an effective description of non-perturbative effects in the gluon-proton interaction. The vector diquark produces the spin-flip effects in the proton coupling with gluon.

It have been shown in [25] that the leading contribution like  $\alpha_s [\alpha_s \ln(1/x)]^n$  to the Pomeron is determined by the gluon ladder graphs. In the  $[\alpha_s]^2$  order we have in the model two ladder graphs shown in Fig. 1 which have  $\alpha_s^2 \ln(1/x)$  behavior. We include to the gluons coupling with the proton the gluon ladder, except two upper  $t$ -channel gluons in Fig. 1. This coupling is shown in the graphs of Fig. 1 by the blob. In what follows we shall calculate the imaginary part of the Pomeron contribution to the scattering amplitude which dominates in the high-energy region. This contribution is equivalent to the  $t$ -channel cut in the gluon-loop graphs. In the diquark model the following structures in the coupling appears

$$V_{pgg}^{\alpha\beta}(p, t, x_P, l_\perp) = B(t, x_P, l_\perp)(\gamma^\alpha p^\beta + \gamma^\beta p^\alpha) + \frac{iK(t, x_P, l_\perp)}{2m}(p^\alpha \sigma^{\beta\gamma} r_\gamma + p^\beta \sigma^{\alpha\gamma} r_\gamma) + iD(t, x_P, l_\perp) \epsilon^{\alpha\beta\delta\rho} p_\delta \gamma_\rho \gamma_5 + \dots \quad (11)$$

In the matrix structure here we have wrote only the terms which have the maximal powers of large proton momentum  $p$ . The structure functions in (11) is dependent over the transverse part of the gluon momentum  $l_\perp$ . The first two terms of the vertex (11) are symmetric in the gluon indices  $\alpha, \beta$ . The structure proportional to  $B(t, \dots)$  determines the spin-non-flip contribution. The term  $\propto K(t, \dots)$  leads to the transverse spin-flip in the vertex. The asymmetric structure in (11) is proportional to  $D \gamma_\rho \gamma_5$  and can be associated with  $\Delta G$ . It should give a visible contribution to the double spin longitudinal asymmetry  $A_{ll}$ . We do not consider this structure in this paper and concentrate in transverse effects in the proton. In a QCD-based diquark model of the proton, the structure (11) of the proton coupling with a two-gluon system has been calculated for moderate momentum transfer [26]. At small momentum transfer such model calculation is not possible and we do not know explicitly the functions  $B, K, \dots$  in (11). Note that the coupling similar to (11) has been found in high energy quark-quark scattering when the large-distance effects has been considered in the gluon loops [27].

In what follows we consider interaction of gluons from Pomeron with quarks produces

by the  $\gamma^* \rightarrow Q\bar{Q}$  transition. The typical momentum of quarks is proportional to the photon momentum  $q$ . In Feynman gauge we can decompose the  $g_{\mu\nu}$  tensors from  $t$ -channel gluons into the longitudinal and transverse parts [25].

$$g^{\alpha\alpha'} = g_l^{\alpha\alpha'} + g_{\perp}^{\alpha\alpha'} \text{ with } g_l^{\alpha\alpha'} \sim \frac{p^\alpha p^{\alpha'}}{(pq)}. \quad (12)$$

The product of the  $g_l^{\alpha\alpha'}$  tensors with the two-gluon coupling with the proton can be written in the form

$$g_l^{\alpha'\alpha} g_l^{\beta'\beta} V_{pgg}^{\alpha\beta}(p, t, x_P, l_{\perp}) \propto p^{\alpha'} p^{\beta'} \left[ \frac{q}{(pq)} B(t, x_P, l_{\perp}) + \frac{iK(t, x_P, l_{\perp})}{2m(pq)} \sigma^{\beta\gamma} q_{\beta} r_{\gamma} \right]. \quad (13)$$

The structure proportional to  $D$  is asymmetric over gluon indexes. It will contribute only in the case when one gluon tensor has transverse component. It can be seen that the structure in square brackets in (13) is related directly to the definitions of the skewed gluon distribution (see e.g. [1]). So, one can conclude that after integration over the gluon transverse momentum  $l_{\perp}$  we should have connections:

$$\begin{aligned} \mathcal{F}_{\zeta}^g(\zeta, t) &\propto \int d^2 l_{\perp} B(t, \zeta = x_P, l_{\perp}) \phi(l_{\perp}, \dots) \\ \mathcal{K}_{\zeta}^g(\zeta, t) &\propto \int d^2 l_{\perp} K(t, \zeta = x_P, l_{\perp}) \phi(l_{\perp}, \dots), \end{aligned} \quad (14)$$

and  $B$  and  $K$  are unintegrated gluon distribution functions which describes spin-average and transverse spin effects in the proton. The universal function  $\phi$  in (14) will be found later. In realistic calculation we use  $g^{\alpha\alpha'}$  tensor without its decomposition into longitudinal and transverse parts.

The hadronic tensor is given by

$$W^{\alpha\alpha';\beta\beta'}(s_p) = \sum_{\text{spin } s_f} \bar{u}(p', s_f) V_{pgg}^{\alpha\alpha'}(p, t, x_P, l) u(p, s_p) \bar{u}(p, s_p) V_{pgg}^{\beta\beta'}(p, t, x_P, l') u(p', s_f). \quad (15)$$

The spin-average and spin-dependent hadron tensors are determined as

$$W^{\alpha\alpha';\beta\beta'}(\pm) = \frac{1}{2} (W^{\alpha\alpha';\beta\beta'}(+s_p) \pm W^{\alpha\alpha';\beta\beta'}(-s_p)). \quad (16)$$

This form is written for arbitrary spin vector  $s_p$  and can be used as well for transversally or longitudinally polarized target. In the last case the contribution of  $D$  structure should be considered. For the leading term of spin-average structure  $W(+)$  for the ansatz (11) we find

$$W^{\alpha\alpha';\beta\beta'}(+) = 16p^{\alpha} p^{\alpha'} p^{\beta} p^{\beta'} (|B|^2 + \frac{|t|}{m^2} |K|^2). \quad (17)$$

Note that we omit for simplicity here and in what follows the arguments of the  $B$  and  $K$  functions unless it is necessary. However, we shall remember that the amplitudes  $B$  and  $K$  depend on  $l$ , otherwise the complex conjugate values  $B^*$  and  $K^*$  are the functions of  $l'$ . The obtained equation for the spin-average tensor coincide in form with the cross section of the proton off the spinless particle (meson e.g.). Really, the meson–proton helicity-non-flip and helicity-flip amplitudes can be written in terms of the invariant functions  $\tilde{B}$  and  $\tilde{K}$  which describe spin-non-flip and spin-flip effects

$$F_{++}(s, t) = is[\tilde{B}(t)]f(t); \quad F_{+-}(s, t) = is\frac{\sqrt{|t|}}{m}\tilde{K}(t)f(t), \quad (18)$$

where  $f(t)$  is determined by the Pomeron coupling with meson. The cross-section is written in the form

$$\frac{d\sigma}{dt} \sim [|\tilde{B}(t)|^2 + \frac{|t|}{m^2}|\tilde{K}(t)|^2]f(t)^2. \quad (19)$$

The term proportional to  $\tilde{B}$  represents the standard Pomeron coupling that leads to the non-flip amplitude. The  $\tilde{K}$  function is the spin-dependent part of the Pomeron coupling which produces in our case the not vanishing at high-energies spin-flip effects. The models [26, 28] predict the value of single spin transverse asymmetry of about 10% for  $|t| \sim 3\text{GeV}^2$  which is of the same order of magnitude as that observed experimentally [29]. It has been found in [26, 28] that the ratio  $|\tilde{K}|/|\tilde{B}| \sim 0.1\text{--}0.2$  and has a weak energy dependence. The weak energy dependence of spin asymmetries in exclusive reactions is not in contradiction with the experiment [28, 30].

The spin-dependent part of the hadron tensor can be written as

$$W^{\alpha\alpha';\beta\beta'}(-) = S_0^{\alpha\alpha';\beta\beta'} + S_r^{\alpha\alpha';\beta\beta'} + A_t^{\alpha\alpha';\beta\beta'}. \quad (20)$$

The functions  $S$  are symmetric in  $\alpha, \alpha'$  and  $\beta, \beta'$  indices

$$S_0^{\alpha\alpha';\beta\beta'} = 8i\frac{BK^* - B^*K}{m}p^\beta p^{\beta'}\Gamma^{\alpha\alpha'} \quad (21)$$

and

$$\begin{aligned} S_r^{\alpha\alpha';\beta\beta'} &= 2i\frac{B^*K}{m}\left(p^\alpha(r_P)^{\alpha'} + p^{\alpha'}(r_P)^\alpha\right)\Gamma^{\beta\beta'} \\ &- 2i\frac{BK^*}{m}\left(p^\beta(r_P)^{\beta'} + p^{\beta'}(r_P)^\beta\right)\Gamma^{\alpha\alpha'} \end{aligned} \quad (22)$$

Here

$$\Gamma^{\alpha\alpha'} = p^\alpha\epsilon^{\alpha'\gamma\delta\rho}p_\gamma(r_P)_\delta(s_p)_\rho + p^{\alpha'}\epsilon^{\alpha\gamma\delta\rho}p_\gamma(r_P)_\delta(s_p)_\rho \quad (23)$$

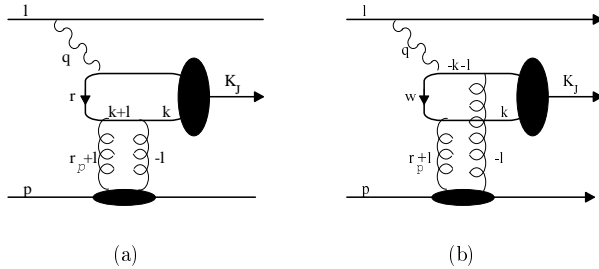


Figure 2: Two-gluon contribution to the diffractive vector meson production..

The function  $A_t$  has asymmetric part

$$A_t^{\alpha\alpha';\beta\beta'} = 2i|t|\frac{B^*K}{m} \left[ p^\alpha p^\beta \epsilon^{\alpha'\beta'\delta\rho} p_\delta(s_p)_\rho + p^\alpha p^{\beta'} \epsilon^{\alpha'\beta\delta\rho} p_\delta(s_p)_\rho + p^{\alpha'} p^\beta \epsilon^{\alpha\beta'\delta\rho} p_\delta(s_p)_\rho + p^{\alpha'} p^{\beta'} \epsilon^{\alpha\beta\delta\rho} p_\delta(s_p)_\rho \right] \quad (24)$$

Note, that this forms are general and can be used for different polarization vectors of the proton. For longitudinal proton polarization the structure  $D$  should be included.

## 4 Diffractive Vector Meson Leptoproduction

Now we are passing to analyses of the amplitude of the vector meson production through the photon-two gluon fusion. In what follows we have regarded mainly the  $J/\Psi$  meson production. This meson can be considered as an  $S$ -wave system of heavy  $c\bar{c}$  quarks [31]. The  $J/\Psi$ -wave function in this case has a form  $g(\not{k} + m_c)\gamma_\mu$  where  $k$  is the momentum of quark and  $m_c$  is its mass. In the nonrelativistic approximation both the quarks have the same momenta  $k$  equal to half of the vector meson momentum  $K_J$  and the mass of  $c$  quark is equal to  $m_J/2$ . The transverse quark motion does not considered. This means that the vector meson wave function is approximated by the simple form  $\delta(\tau - 1/2)\delta(k_t^2)$ . The constant  $g$  in the wave function can be expressed through the  $e^+e^-$  decay width of the  $J/\Psi$  meson

$$g^2 = \frac{3\Gamma_{e^+e^-}^J m_J}{64\pi\alpha^2}. \quad (25)$$

It is known (see [10, 11] e.g.) that the leading terms of the amplitude of the diffractive vector meson production is mainly imaginary. We shall consider here only the imaginary parts of the amplitudes. In this case only graph of Fig.2 contribute. The gluons from the Pomeron are coupled with the single and different quarks in the  $c\bar{c}$  loop (see Fig. 2 a, b).

To calculate the imaginary part of the amplitude we must consider the  $\delta$ -function contribution in the  $s$ -channel propagators ( $k + l$  and  $p' - l$  lines for Fig 2 a). With the help of the  $\delta$  functions the integration over  $l$

$$\int d^4l = \frac{1}{2} \int dl_+ dl_- dl_\perp \quad (26)$$

can be carried out over  $l_+$  and  $l_-$  variables. One can find that both the  $l_\pm$  components of the vector  $l$  are small:  $l_+ \sim l_- \propto 1/p_+$ . This results in the transverse of the gluon momentum  $l^2 \simeq -l_\perp^2$ . The same is true for integration over  $l$  in the nonplanar graph of Fig 2. b. For the arguments in the off mass shell quark propagators of Fig 2. a, b, we find

$$\begin{aligned} r^2 - m_c^2 &= -\frac{M_J^2 + Q^2 + |t|}{2}, \\ w^2 - m_c^2 &= -2 \left( l_\perp^2 + \vec{l}_\perp \vec{r}_\perp + \frac{M_J^2 + Q^2 + |t|}{4} \right). \end{aligned} \quad (27)$$

Thus these quark lines are far from the mass shell for heavy vector meson production even for small  $Q^2$  [10].

We calculate here directly polarized cross section of vector meson production. Cross section can be represented as a squared of  $\gamma^* gg \rightarrow V$  amplitude convoluted with the lepton and hadron polarized tensors. Some details of calculations which was done for longitudinal target polarization can be found in [32]. We consider both longitudinal and transverse polarization of vector meson and suppose the same form of wave function in these cases. For the sum over polarization for  $J/\Psi$  polarized vectors  $e_J$  we have

$$\sum_{Spin_J} e_J^\rho (e_J^\sigma)^+ = -g^{\rho\sigma} + \frac{K_J^\rho K_J^\sigma}{m_J^2}. \quad (28)$$

The spin-average and spin-dependent cross-sections of the vector meson leptoproduction with longitudinal polarization of a lepton and opposite transverse polarization of the proton are determined by the relation

$$d\sigma(\pm) = \frac{1}{2} (d\sigma(\rightarrow \uparrow) \pm d\sigma(\rightarrow \downarrow)). \quad (29)$$

The cross section  $d\sigma(\pm)$  can be written in the form

$$\frac{d\sigma^\pm}{dQ^2 dy dt} = \frac{|T^\pm|^2}{32(2\pi)^3 Q^2 s^2 y}. \quad (30)$$

For the spin-average amplitude square we find

$$|T^+|^2 = s^2 N \left( (1 + (1 - y)^2) m_V^2 + 2(1 - y) Q^2 \right) \left[ |\tilde{B}|^2 + |\tilde{K}|^2 \frac{|t|}{m^2} \right]. \quad (31)$$

Here  $N$  is a normalization factor

$$N = \frac{\Gamma_{e^+e^-}^J M_J \alpha_s^4}{27\pi^2}. \quad (32)$$

The term proportional to  $(1+(1-y)^2)m_V^2$  represents the contribution of the virtual photon with transverse polarization. The  $2(1-y)Q^2$  term describes the effect of longitudinal photons. This contribution is predominant for high  $Q^2$ . The  $\tilde{B}$  and  $\tilde{K}$  functions are expressed through the integral over transverse momentum of the gluon. The function  $\tilde{B}$  is determined by

$$\begin{aligned} \tilde{B} &= \frac{1}{4\bar{Q}^2} \int \frac{d^2 l_\perp (l_\perp^2 + \vec{l}_\perp \vec{\Delta}) B(t, l_\perp^2, x_P, \dots)}{(l_\perp^2 + \lambda^2)((\vec{l}_\perp + \vec{\Delta})^2 + \lambda^2)[l_\perp^2 + \vec{l}_\perp \vec{\Delta} + \bar{Q}^2]} \\ &\sim \frac{1}{4\bar{Q}^4} \int_0^{l_\perp^2 < \bar{Q}^2} \frac{d^2 l_\perp (l_\perp^2 + \vec{l}_\perp \vec{\Delta})}{(l_\perp^2 + \lambda^2)((\vec{l}_\perp + \vec{\Delta})^2 + \lambda^2)} B(t, l_\perp^2, x_P, \dots), \end{aligned} \quad (33)$$

with  $\bar{Q}^2 = (m_V^2 + Q^2 + |t|)/4$ . This is modification of the scale variable proposed in [10, 11] to the case of large momentum transfer. The term  $(l_\perp^2 + \vec{l}_\perp \vec{\Delta})$  appears in the numerator of (33) because of the cancellation between the planar and nonplanar graphs where gluons are coupled with the single and different quarks (Fig.2). The  $\tilde{K}$  function is determined by a similar integral. The integral (33) can be connected with the gluon SPD as

$$\mathcal{F}_{x_P}^g(x_P, t, \bar{Q}^2) = \int_0^{l_\perp^2 < \bar{Q}^2} \frac{d^2 l_\perp (l_\perp^2 + \vec{l}_\perp \vec{\Delta})}{(l_\perp^2 + \lambda^2)((\vec{l}_\perp + \vec{\Delta})^2 + \lambda^2)} B(t, l_\perp^2, x_P, \dots) \propto \tilde{B}. \quad (34)$$

Note that if one consider effects of the transverse quark motion in the the vector meson wave function, the scale variable in SPD will be changed to  $\bar{Q}^2 \rightarrow \bar{Q}^2 + k_\perp^2$  [12, 33]. Thus, the  $B(l_\perp^2, x_P, \dots)$  function is the nonintegrated spin- average gluon distribution. The  $\tilde{K}$  function is proportional to the  $\mathcal{K}_{x_P}^g(x_P, t)$  distribution. The function  $\phi$  in (14) has the form

$$\phi(l_\perp, \dots) = \frac{(l_\perp^2 + \vec{l}_\perp \vec{\Delta})}{(l_\perp^2 + \lambda^2)((\vec{l}_\perp + \vec{\Delta})^2 + \lambda^2)}. \quad (35)$$

The spin-dependent amplitude square looks like

$$|T^-|^2 = s|t|N \frac{\vec{Q} \vec{S}_\perp}{4m} (Q^2 + m_V^2 + |t|) \frac{\tilde{B} \tilde{K}^* + \tilde{B}^* \tilde{K}}{2}. \quad (36)$$

We shall use the spin-dependent cross sections obtained here for the numerical analyses of polarized vector meson production in section 6.

## 5 Diffractive $Q\bar{Q}$ Photoproduction

Let us study now the diffractive  $Q\bar{Q}$  production in the lepton-proton reaction. This process is determined by similar graphs shown in Fig. 2. The change is in the photon-two-gluon fusion amplitude where we do not project the  $Q\bar{Q}$  state to the vector meson. The quark-antiquark contribution instead  $t$ -channel gluons is possible for light quark production. To suppress this contribution of quark structure function which should be essential at large  $x$ , we investigate quark production at small  $x \leq 0.1$ . In this kinematical region the gluon contribution is predominated.

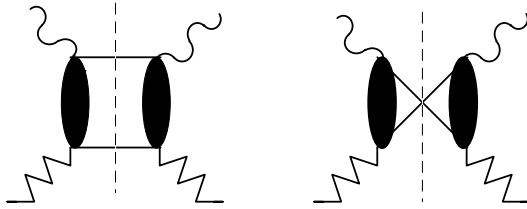


Figure 3: Box graphs contribution to the cross section of diffractive  $Q\bar{Q}$  production.

As in the case of vector meson production we calculate spin average and spin-dependent cross section (30) of the diffractive  $Q\bar{Q}$  lepto production. To calculate these cross sections we must integrate corresponding amplitudes squared over the  $Q\bar{Q}$  phase space  $dN_{Q\bar{Q}} = \Pi_f \frac{d^3 p_f}{(2\pi)^3 2E_f}$  with delta function which reflect the momentum conservation. It can be easily seen that

$$\frac{d^3 p_1}{2E_1} \frac{d^3 p_2}{2E_2} \delta^4(q + r_P - p_1 - p_2) = d^4 p_1 \delta(p_1^2 - m_q^2) \delta(p_2^2 - m_q^2) \quad (37)$$

and the calculation of  $\gamma gg \rightarrow Q\bar{Q}$  cross section is equivalent to computation of imaginary part of quark loop diagram shown in Fig.3. The amplitude of photon-two-gluon fusion shown by the blobs in Fig.3 represents the sum of graphs in Fig.4. The diagrams of Fig.4 are similar to the planar and nonplanar gluon graphs of Fig.2. As a result, the gluon contribution to the cross section should be similar to obtained in (33).

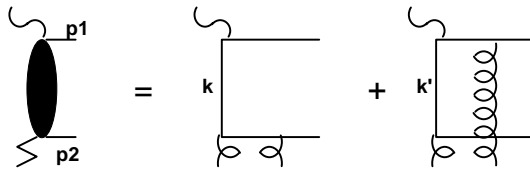


Figure 4: The amplitude of photon-two-gluon fusion

The final quark momenta  $p_1$ ,  $p_2$  and the momentum of the off-mass-shell quark  $k$  ( $k'$ ) can be determined with the help of delta functions in (37). There are two solutions for

the vectors. We find for Solution 1, that  $p_1 \sim q$  and  $p_2 \sim r_P$  and vector  $k$  is mainly transversal:  $k^2 \sim -k_\perp^2$ . For Solution 2 the quarks momentum changed places  $p_1 \leftrightarrow p_2$ . In this case vector  $k$  has large longitudinal component and  $k^2 \sim -x_P p_+^2$ . One can suppose that such contributions should be suppressed. However, in this case we find similar large variable from trace in numerator of the diagram that compensate  $p_+^2$  in denominator. As a result, both integration regions for Solution 1 and Solution 2 contribute to the cross section. Similar compensation between numerator and denominator takes place for the nonplanar quark loop diagrams (second graph in Fig.3). In this case we have large variable only in one propagator. The calculation of the  $\gamma gg \rightarrow Q\bar{Q}$  process is more complicated with respect to vector meson case. We must consider here 8 graphs with two solutions for quark momenta.

The integration over quark momenta  $k_\pm$  in the loop can be done with the help of delta functions in (37)

$$d^4k \delta(p_1^2 - m_q^2) \delta(p_2^2 - m_q^2) \sim \frac{d^2 k_\perp}{\sqrt{M_X^2 - 4(k_\perp^2 + m_q^2)}} \quad (38)$$

As a result, the spin-average and spin-dependent cross section can be written in the form

$$\frac{d^5\sigma(\pm)}{dQ^2 dy dx_p dt dk_\perp^2} = \binom{(2-2y+y^2)}{(2-y)} \frac{C(x_P, Q^2) N(\pm)}{\sqrt{1 - 4(k_\perp^2 + m_q^2)/M_X^2}}. \quad (39)$$

Here  $C(x_P, Q^2)$  is a normalization function which is common for the spin average and spin dependent cross section;  $N(\pm)$  is determined by the sum of graphs in Fig.3,4 integrated over the gluon momenta  $l$  and  $l'$ .

$$N(\pm) = \int \frac{d^2 l_\perp d^2 l'_\perp (l_\perp^2 + \vec{l}_\perp \vec{\Delta}) ((l'_\perp)^2 + \vec{l}'_\perp \vec{\Delta}) D^\pm(t, Q^2, l_\perp, l'_\perp, \dots)}{(l_\perp^2 + \lambda^2)((\vec{l}_\perp + \vec{r}_\perp)^2 + \lambda^2)(l'_\perp^2 + \lambda^2)((\vec{l}'_\perp + \vec{r}'_\perp)^2 + \lambda^2)} \quad (40)$$

The  $D^\pm$  function here is a sum of traces over the quark loops of the graphs in Fig.3,4 and corresponding crossed diagrams convoluted with the spin average and spin-dependent tensors. The calculation shows a considerable cancellation between the planar and nonplanar contribution of the graphs in Fig.4. As a result, the function  $D^\pm$  in (40) is proportional to the gluon momenta  $l_\perp$  and  $l'_\perp$  as in the case of vector meson production (33).

The contribution of planar graph of Fig.4 to  $D(+)$  has the following form

$$D^p(+) = \left( |B|^2 + |t|/m^2 |K|^2 \right) \left( (k_\perp + r_\perp)^2 + m_q^2 \right) F(k_\perp, l_\perp), \quad (41)$$

where

$$F(k_\perp, l_\perp) = \frac{1}{\left( k_\perp^2 + m_q^2 \right)^2 \left( (k_\perp - l_\perp)^2 + m_q^2 \right) \left( (k_\perp - l'_\perp)^2 + m_q^2 \right)}. \quad (42)$$

This function contains production of the off-mass-spell quark propagators in the graphs Fig. 3, 4. We see that the quark virtuality here is quite different with respect to the vector meson case. We do not have here the terms proportional to  $Q^2$  as in (27).

This will change the scale in corresponding gluon structure functions. Really, denominators in (42) determine the effective integration region over  $l$  and  $l'$  in (32). We can rewrite approximately the contribution of  $D^p(+)$  to  $N(+)$

$$N^p(+) \sim \frac{(\tilde{B}|^2 + |t|/m^2|\tilde{K}|^2) \left( (k_\perp + r_\perp)^2 + m_q^2 \right)}{\left( k_\perp^2 + m_q^2 \right)^4} \quad (43)$$

with

$$\tilde{B} \sim \int_0^{l_\perp^2 < k_0^2} \frac{d^2 l_\perp (l_\perp^2 + \vec{l}_\perp \vec{\Delta})}{(l_\perp^2 + \lambda^2)((\vec{l}_\perp + \vec{\Delta})^2 + \lambda^2)} B(t, l_\perp^2, x_P, \dots) = \mathcal{F}_{x_P}^g(x_P, t, k_0^2). \quad (44)$$

and

$$\tilde{K} \sim \int_0^{l_\perp^2 < k_0^2} \frac{d^2 l_\perp (l_\perp^2 + \vec{l}_\perp \vec{\Delta})}{(l_\perp^2 + \lambda^2)((\vec{l}_\perp + \vec{\Delta})^2 + \lambda^2)} K(t, l_\perp^2, x_P, \dots) = \mathcal{K}_{x_P}^g(x_P, t, k_0^2) \quad (45)$$

with  $k_0^2 \sim k_\perp^2 + m_q^2$ . This scale is similar to found in [18]. As we expected, the gluon structure functions are determined by the same integrals as in (34) but with different scale.

The function  $N(+)$  in the spin-average cross section which has contribution of all graphs can be written as

$$N(+) = \left( |B|^2 + |t|/m^2 |K|^2 \right) \Pi^{(+)}(t, k_\perp^2, Q^2) \quad (46)$$

It was mentioned above that there are graphs with large quark virtuality. Propagators of these lines become pointlike. As a result graphs in the integration region for Solution 1 and Solution 2 have different  $Q^2$  dependence. This results in the nontrivial  $Q^2$  behavior of  $\Pi^{(+)}$ . The function  $\Pi^{(+)}$  is complicated in form and will be calculated numerically.

The calculation of spin-dependent cross section is more complicated. In addition to the term observed in (36) and proportional to the scalar production  $\vec{Q} \vec{S}_\perp$  the additional term  $\propto \vec{k}_\perp \vec{S}_\perp$  appears. Such contribution can not be found in the vector meson production because we must integrate there the amplitudes over  $d^2 k_\perp$ . The function  $N(-)$  has the form

$$N(-) = \frac{t(BK^* + B^*K)}{m^2} \left[ \frac{(\vec{Q} \vec{S}_\perp)}{m} \Pi_Q^{(-)}(t, k_\perp^2, Q^2) + \frac{(\vec{k}_\perp \vec{S}_\perp)}{m} \Pi_k^{(-)}(t, k_\perp^2, Q^2) \right]. \quad (47)$$

The functions  $\Pi_{Q(k)}^{(-)}$  will be calculated numerically as the function  $\Pi^{(+)}$ .

## 6 Numerical Results for Vector Meson Leptoproduction

We shall calculate the polarized cross section (29) of the diffractive  $J/\Psi$  production determined by the amplitudes (31, 36). The spin-average cross section of the vector meson production is proportional at small momentum transfer to  $|B|^2$  function (31) which is connected with the skewed gluon distribution (34). This result is in accordance with the imaginary part of the amplitude found on the basis of SPD approach [1]. We use here a simple parameterization of SPD as a product of the form factor and the ordinary gluon distribution

$$B(t, x_P, \bar{Q}^2) = F_B(t) \left( x_P G(x_P, \bar{Q}^2) \right). \quad (48)$$

where for simplicity the form factor  $F_B(t)$  is chosen as the electromagnetic form factor of the proton. Such simple choice can be justified by that the Pomeron–proton vertex might be similar to the photon–proton coupling [34, 35]

$$F_B(t) \sim F_p^{em}(t) = \frac{(4m_p^2 + 2.8|t|)}{(4m_p^2 + |t|)(1 + |t|/0.7GeV^2)^2}. \quad (49)$$

To perform simple estimations we shall use our results from [26, 28] where it was found that the ratio of spin asymmetries in exclusive reactions at small momentum transfer may have a weak energy dependence. The corresponding asymmetries are proportional to the ratio  $|\tilde{K}|/|\tilde{B}|$  at small  $x \sim 1/s$ . We shall suppose that this is true for the ratio of spin dependent and spin average densities in our case too and

$$\frac{|\tilde{K}|}{|\tilde{B}|} \sim 0.1. \quad (50)$$

We shall use this value in our estimation of spin asymmetries of hadron leptoproduction at small  $x$ .

The energy dependence of the cross sections is determined by the Pomeron contribution to the gluon distribution function at small  $x$

$$\left( x_P G(x_P, \bar{Q}^2) \right) \sim \frac{const}{x_P^{1-\alpha_p(t)}} \sim \left( \frac{sy}{m_J^2 + Q^2 + |t|} \right)^{(\alpha_p(t)-1)}. \quad (51)$$

Here  $\alpha_p(t)$  is a Pomeron trajectory which is chosen in the form

$$\alpha_p(t) = 1 + \epsilon + \alpha' t. \quad (52)$$

with  $\epsilon = 0.15$  and  $\alpha' = 0$ . These values are in accordance with the fit of the diffractive  $J/\Psi$  production by ZEUS [36]

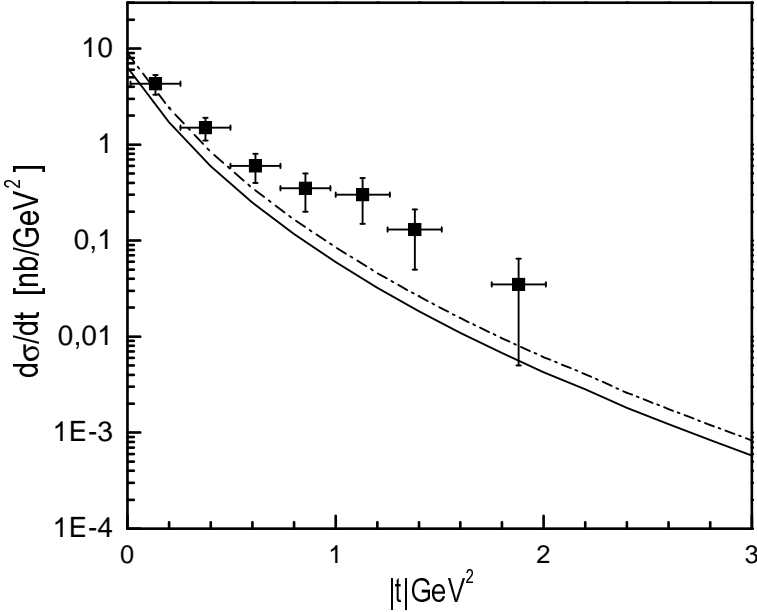


Figure 5: The differential cross section of the  $J/\Psi$  production at HERA energy: solid line -for  $|\tilde{K}|/|\tilde{B}| = 0$ ; dot-dashed line -for  $|\tilde{K}|/|\tilde{B}| = 0.1$ . Data are from [6].

The typical scale of the reaction is determined by  $\bar{Q}^2 = (m_J^2 + Q^2 + |t|)/4$ . For not large  $Q^2$  and  $|t|$  the value of  $\bar{Q}^2$  is about 2.5-3.0  $\text{GeV}^2$ . In this region we can work with fixed  $\alpha_s \sim 0.3$ . An effective gluon mass in (33) is chosen to be equal to  $0.3 \text{ GeV}^2$ . The cross section depends on this parameter weakly. The value of  $\Gamma_{e^+e^-}^J = 5.26 \text{ keV}$  is used. The predicted cross sections are shown in Fig. 5. Our results reproduce experimental data quite well.

The  $A_{LT}$  asymmetry for vector meson production is determined by the ratio of cross sections determined in (36,31)

$$A_{LT} = \frac{\sigma(-)}{\sigma(+)} \sim \frac{\vec{Q} \vec{S}_\perp}{4m} \frac{yx_P|t|}{(1 + (1 - y)^2)m_V^2 + 2(1 - y)Q^2} \frac{\tilde{B} \tilde{K}}{|\tilde{B}|^2 + |\tilde{K}|^2|t|/m^2}. \quad (53)$$

For small momentum transfer this asymmetry can be approximated as

$$A_{LT} \sim C_g \frac{\mathcal{K}_\zeta^g(\zeta)}{\mathcal{F}_\zeta^g(\zeta)} \quad \text{with } \zeta = x_P \quad (54)$$

Simple estimations shows that the coefficient  $C_g(J/\Psi)$  at HERMES energy for  $y = 0.5, |t| = 1 \text{ GeV}^2, Q^2 = 5 \text{ GeV}^2$  is quite small and of about 0.007. To get expected values for coefficients (54) for light vector mesons we use the same Eqn. (53). The used simple model for the wave function predicts weak mass dependence of the gluon contribution to the asymmetry. For the same kinematical variables  $C(\phi) \sim C(\rho) \sim 0.008$ . However, these results are obtained for the nonrelativistic meson wave function of the

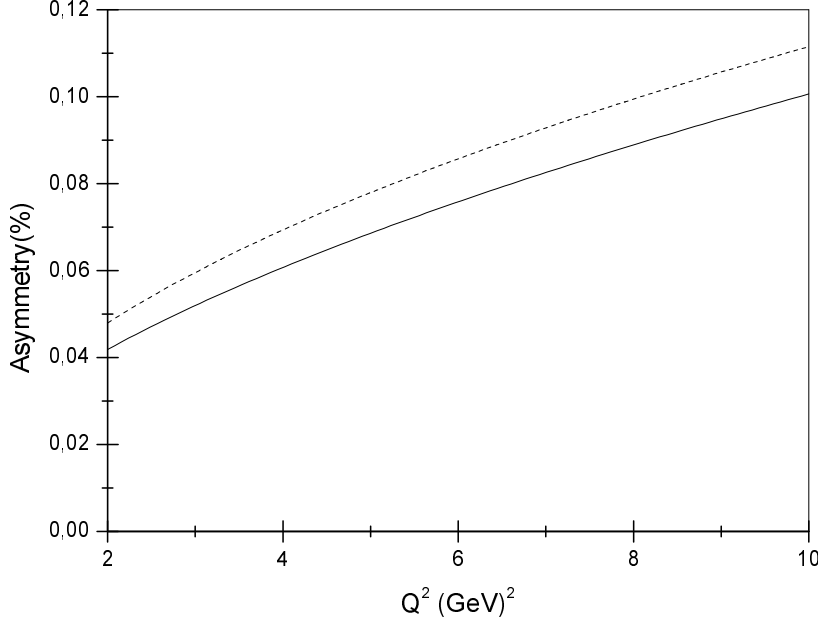


Figure 6: The  $A_{lT}$  asymmetry for vector meson production at HERMES ( $y=0.5$ ,  $|t|=1\text{GeV}^2$ ): solid line -for  $J/\Psi$  production; dotted line -for  $\rho$  production.

form  $\delta(\tau - 1/2)\delta(k_t^2)$  which is not a good approximation for light meson production. To get a suitable predictions for  $\rho, \phi$  meson production it is important to study more realistic wave function and take into consideration the transverse quark degrees of freedom. Moreover, for  $\rho, \phi$  meson production the contribution of quark SPD should be considered in HERMES energy range.

The asymmetry predicted for  $J/\Psi$  production at HERMES energies is shown in Fig. 6 ( $\tilde{K}/\tilde{B} = 0.1$ ) for the case when the transverse part of photon momentum is parallel to the target polarization  $S_\perp$ . Simple estimations on the basis of (54) for  $\rho$  meson production are shown there too. At HERA energies, asymmetry will be extremely small.

## 7 Predictions for $Q\bar{Q}$ Leptoproduction

We shall discuss here our prediction for diffractive  $Q\bar{Q}$  production. We do not consider the cross section but only the asymmetry  $A_{lT} = \sigma(-)/\sigma(+)$ . It is not necessary in this case to include in calculation the factors which are common for individual cross sections and cancel in the ratio. As it was mentioned previously, the spin-dependent contribution has two independent terms proportional to the scalar productions  $\vec{k}_\perp \vec{S}_\perp$  and  $\vec{Q} \vec{S}_\perp$  (47). Let us analyze now the first contribution for the case when the transverse jet momentum  $\vec{k}_\perp$  is parallel to the target polarization  $\vec{S}_\perp$ . The asymmetry is maximal in this case. We would

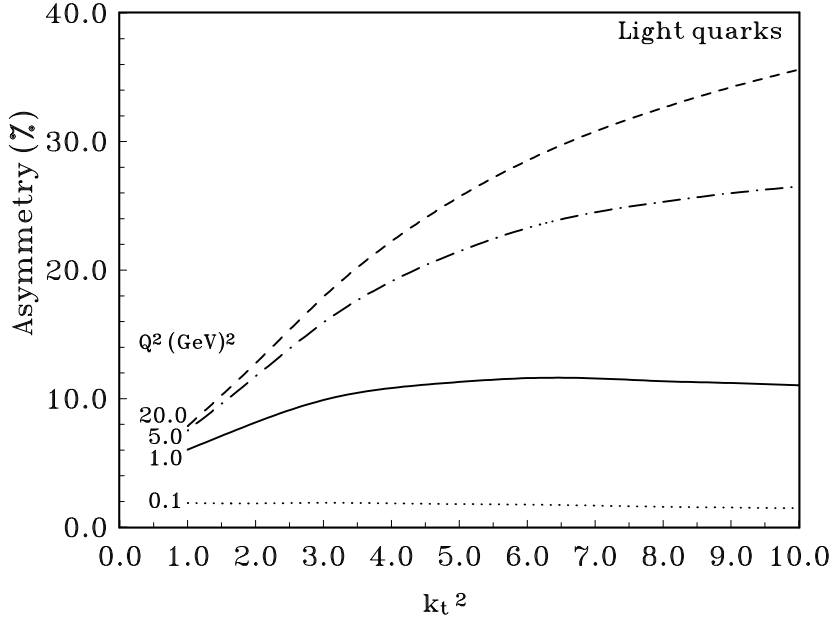


Figure 7: The  $A_{lT}$  asymmetry in diffractive light  $Q\bar{Q}$  production at HERA energies for  $x_P = 0.1$ ,  $y = 0.5$ ,  $|t| = 1(GeV)^2$ .

like to emphasize here that to observe this contribution to asymmetry it is necessary to distinguish experimentally the quark and antiquark jets. This can be done presumably by the charge of the leading particles in the jet which should be connected in charge with the quark produced in photon-gluon fusion. This is indispensable condition in experimental study of such asymmetry caused by the fact that the transverse momentum of quark and antiquark produced in the process are opposite in sign. If we do not separate events with  $\vec{k}_\perp$  for quark jet e.g., the resulting asymmetry will be zero.

As in the case of vector meson production the asymmetry is approximately proportional to the ratio of polarized and spin average gluon distribution functions

$$A_{lT}^{Q\bar{Q}} \sim C^{Q\bar{Q}} \frac{\mathcal{K}_\zeta^g(\zeta)}{\mathcal{F}_\zeta^g(\zeta)} \quad \text{with } \zeta = x_P \quad (55)$$

As previously, we use in our estimations the value  $|\tilde{K}|/|\tilde{B}| \sim 0.1$ . The spin-dependent cross section is vanished for  $Q^2 \rightarrow 0$  while spin-average cross section is constant in this limit. As a result the asymmetry can be estimated as  $A_{lT} \propto Q^2/(Q^2 + Q_0^2)$  with  $Q_0^2 \sim 1\text{GeV}^2$ . The  $Q^2$  dependence of calculated asymmetry for light quark production at HERA energies is shown in Fig. 7. Similar calculation has been done for heavy  $c\bar{c}$  production. The predicted asymmetry is approximately the same as for the light quark production (Fig.8).

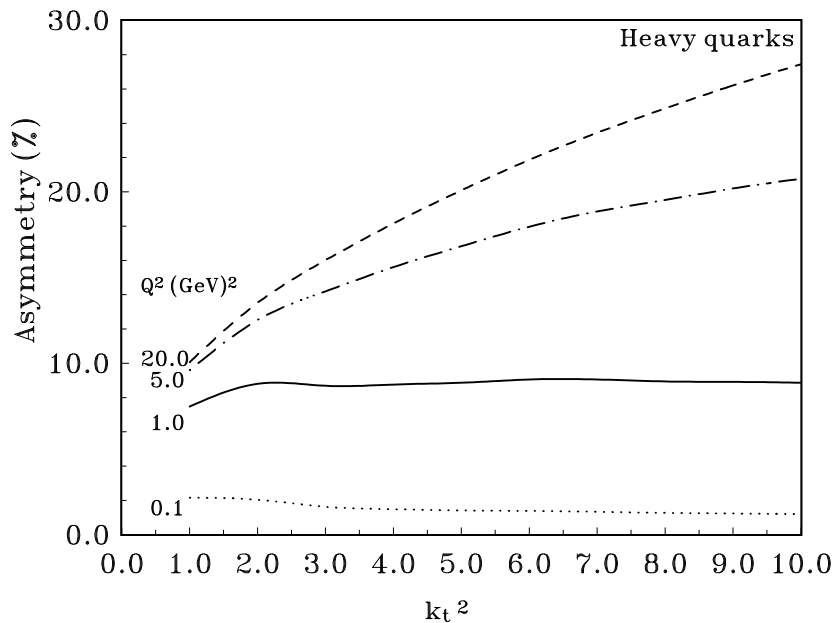


Figure 8: The  $A_{lT}$  asymmetry in diffractive heavy  $Q\bar{Q}$  production at HERA energies for  $x_P = 0.1$ ,  $y = 0.5$ ,  $|t| = 1(GeV)^2$ .

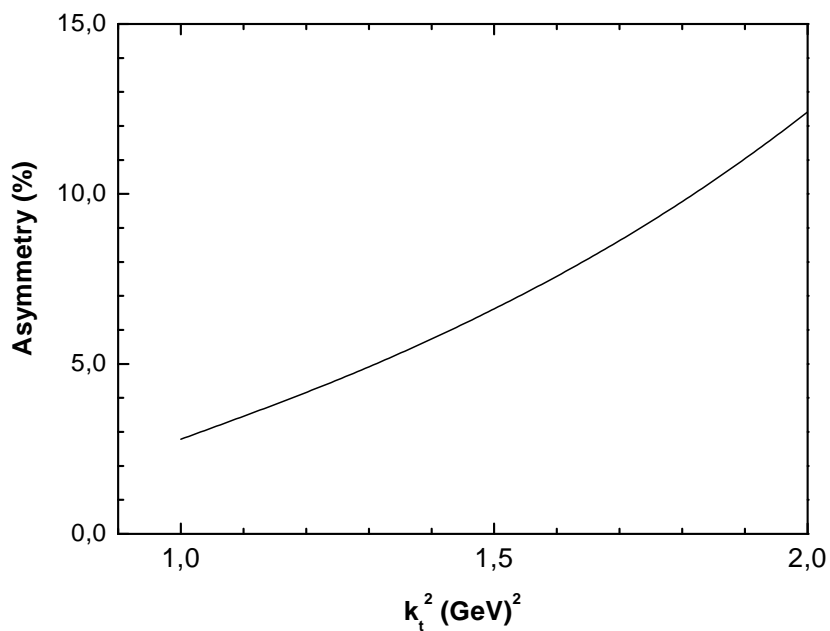


Figure 9: The  $A_{lT}$  asymmetry in diffractive light  $Q\bar{Q}$  production for  $Q^2 = 5\text{GeV}^2$ ,  $x_P = 0.1$ ,  $y = 0.5$ ,  $|t| = 1(GeV)^2$  at HERMES energies.

At the HERMES energies it is not so easy to study perturbative region for  $Q\bar{Q}$  production. Really,  $k_\perp^2$  should be large enough to have a large scale  $k_0^2$  in the process (45). Otherwise we have from (38) restriction that  $k^2 \leq M_X^2/4 = (x_{Pys} + Q^2)/4$ . We find that  $(k_\perp^2)_{max} \sim 2\text{GeV}^2$  for  $x_P = 0.1$ ,  $y = 0.5$  and  $Q^2 = 5\text{GeV}^2$ . This means that we can work only in very limited region of  $k^2$  at HERMES energies. The expected  $A_{lT}$  asymmetry for light quark production at HERMES is shown in Fig.9. We find that for  $k_\perp^2 = 1.5\text{GeV}^2$ ,  $Q^2 = 5\text{GeV}^2$ ,  $x_P = 0.1$ ,  $y = 0.5$  and  $|t| = 1(\text{GeV})^2$  the coefficient  $C^{Q\bar{Q}}$  in (55) is quite large at HERMES energy, about 0.7. This show a possibility to study the polarized gluon distribution  $\mathcal{K}_\zeta^g(x)$  at HERMES experiment.

## 8 Conclusion

In the present paper, the diffractive hadron lepton production for longitudinally polarized lepton and transversally polarized proton at high energies has been studied within the two-gluon exchange model. This means that our results should be applicable for reactions which include heavy quarks. For processes with light quarks, our predictions should be valid in high energy range or small  $x$  region ( $x \leq 0.1$  e.g.) where the contribution of quark SPD is expected to be small.

The polarized cross sections of diffractive hadron production are determined in terms of the leptonic and hadronic tensors and the squared amplitude of the hadron production, through the photon-two-gluon fusion. The hadronic tensor is expressed in terms of the two-gluon coupling with the proton which has the helicity flip part. This gluon coupling with the proton is related with SPD. As a result the cross sections of diffractive meson and  $Q\bar{Q}$  production are expressed in terms of similar integrals which are connected with the gluon SPD  $\mathcal{F}_\zeta(x)$  and  $\mathcal{K}_\zeta(x)$ . The modified scale variable  $\bar{Q}^2 = (m_V^2 + Q^2 + |t|)/4$  is proposed for the vector meson production with large momentum transfer.

The  $A_{lT}$  asymmetry is found to be proportional to the ratio of  $\mathcal{K}/\mathcal{F}$  structure functions and generally can be used to get information on the transverse distribution  $\mathcal{K}_{x_P}^g(x_P, t)$  from experiment. There are some difficulties here. The asymmetry for vector meson production is expected to be quite small  $A_{lT} < 0.1\%$  at HERMES energy range. Similar asymmetry for  $Q\bar{Q}$  production is predicted to be about 10%. It is an excellent object to study transverse effects in the proton coupling with gluons. However, the experimental study of this asymmetry is not so simple. To find nonzero asymmetry in this case, it is necessary to distinguish quark and antiquark jets and to have possibility to study azimuthal asymmetry structure. This is important, because cross sections integrated

over  $d\phi_{Jet}$  are equal to zero. Note, that asymmetry of the same order of magnitude was predicted for diffractive  $Q\bar{Q}$  production in polarized proton- proton interaction [37].

Note that very different result for asymmetry in the cases of vector meson and  $Q\bar{Q}$  production is caused by the following. Generally, in the  $A_{lT}$  asymmetry we have two different terms proportional to the scalar productions  $\vec{k}_\perp \vec{S}_\perp$  and  $\vec{Q} \vec{S}_\perp$  (47). The term  $\propto \vec{k}_\perp \vec{S}_\perp$  does not proportional to small  $x_P$  variable and produces quite large contribution to the asymmetry. This term does not appear in the case of vector meson production because we must integrate there over  $d^2k$ . The second term  $\propto \vec{Q} \vec{S}_\perp$  has  $x_P$  suppression and gives small contribution to the asymmetry of the vector meson and  $Q\bar{Q}$  production.

In the case of the  $\rho$  production, the polarized quark SPD might be studied together with the gluon distribution for  $x \geq 0.1$  at the HERMES experiments. In the case of the  $\phi$  production the strange quark SPD might be analyzed. Similar experiments can be done in future COMPASS spectrometer if transversally polarized target will be constructed there. We conclude that important information on the spin-dependent SPD at small  $x$  can be obtained from the asymmetries in the diffractive hadron lepton production for longitudinally polarized lepton and transversely polarized hadron targets.

We would like to thank A. Borissov, A. Efremov, P. Kroll, T. Morii, O. Nachtmann, W.-D. Nowak and O. Teryaev for fruitful discussions.

This work was supported in part by the Russian Fond of Fundamental Research, Grant 00-02-16696.

## References

- [1] A.V. Radyushkin, Phys.Rev, D **56**, 5524 (1997).
- [2] X. Ji, Phys.Rev. D **55** 7114 (1997).
- [3] J.C. Collins, L. Frenkfurt, M. Strikman, Phys. Rev. **D56**, 2982 (1997).
- [4] F.E. Low, Phys. Rev. **D12**,163; (1975)  
S. Nussinov, Phys. Rev. Lett. **34**, 1286 (1975).
- [5] ZEUS Collab., J. Breitweg et al., Z. Phys, **C75**, (1997) 215.
- [6] H1 Collaboration, S. Aid et al., Nucl. Phys. **B472**, (1996) 3.
- [7] H1 Collab., C. Adloff et al., Eur. Phys. J. **C10**, 373 (1999).
- [8] ZEUS Collab., J. Breitweg et al., Eur. Phys. J. **C5**, 41 (1998);  
H1 Collab., C. Adloff et al., Eur. Phys. J. **C6** 421 (1999).
- [9] HERMES Collab., A. Airapetian et al, Phys. Lett. **B513**, 301 (2001).
- [10] M.G. Ryskin, Z. Phys. **C57**, 89 (1993).
- [11] S.J. Brodsky at al., Phys. Rev. **D50**, 3134 (1994).
- [12] M.G. Ryskin, R.G. Roberts, A.D. Martin, E.M. Levin, Z. Phys. **C76**, 231 (1997).
- [13] J.L. Cudell, I. Royen, Nucl. Phys. **B545**, 505 (1999);
- [14] D.Y. Ivanov, R. Kirshner, Phys. Rev. **D58**, 114026 (1998).
- [15] L. Mankiewicz, G. Piller, T. Weigl, Eur. Phys. J. **C5**, 119 (1998).
- [16] H.W. Huang, P. Kroll, Eur. Phys. J. **C17**, 423 (2000).
- [17] M. Vänttinen. L. Mankiewicz, Phys.Lett. **B434**, 141 (1998).
- [18] J. Bartels, C. Ewerz, H. Lotter, M.Wüsthoff, Phys. Lett. **B386**, 389 (1975).
- [19] M.Diehl, Z. Phys. **C66**, 181 (1995).
- [20] B. Lehmann-Dronke, M. Maul, S. Schaefer, E.Stein, A. Schäfer, Phys.Lett. **B457**, 207 (1999).
- [21] J. Bartels, T. Gehrmann, M.G. Ryskin, Eur. Phys. J. **C11**, 325 (1999).

- [22] S.V. Goloskokov, Proc. of the 14th International Spin Physics Symposium, SPIN2000, AIP Conference Proc. **V.570**, 541 (hep-ph/0011341); hep-ph/0110212.
- [23] M. Anselmino, A. Efremov, E. Leader, Phys. Rept. **261**, 1 (1995).
- [24] M. Anselmino, P. Kroll, B. Pire, Z. Phys. **C36**, 36 (1987).
- [25] L.V. Gribov, E.M. Levin, M.G. Ryskin, Phys. Rept. **100**, 151 (1983).
- [26] S.V. Goloskokov, P. Kroll, Phys. Rev. D **60**, 014019 (1999).
- [27] S.V. Goloskokov, Phys.Lett. **B315**, 459 (1993).
- [28] S.V. Goloskokov, S.P. Kuleshov, O.V. Selyugin, Z. Phys. **C50**, (1991) 455.
- [29] D.C. Peaslee et al., Phys. Rev. Lett. **51**, 2359 (1983).
- [30] N. Akchurin, S.V. Goloskokov, O.V. Selyugin, Int.J.Mod.Phys. **A14**, 253 (1999).
- [31] E.L. Berger, D. Jones, Phys. Rev. **D23**, 1521 (1981).
- [32] S.V. Goloskokov, Eur. Phys. J. **C11**, 309 (1999).
- [33] S.V. Goloskokov, in Proc. of XV International Seminar on High Energy Physics Problems "Relativistic Nuclear Physics and Quantum Chromodynamics", Dubna September 25-29, 2000; hep-ph/0012307.
- [34] A. Donnachie, P.V. Landshoff, Nucl. Phys. **B244**, (1984) 322.
- [35] T. Arens, M. Diehl, O. Nachtmann, P.V. Landshoff, Z. Phys. **C74**, (1997) 651.
- [36] ZEUS Collab., J. Breitweg et al., Eur. Phys. J. **C14**, 213 (2000).
- [37] S.V. Goloskokov, Phys.Rev. **D53**, 5995 (1996).